Colorimetric and fluorimetric response of salicylaldehyde dithiosemicarbazone towards fluoride, cyanide and copper ions: Spectroscopic and TD-DFT studies

Vengayil K. Harikrishnan, Sabeel M. Basheer, Nithin Joseph, Anandaram Sreekanth

PII: S1386-1425(17)30274-3
DOI: doi: 10.1016/j.saa.2017.04.007
Reference: SAA 15060

To appear in: *Spectrochimica Acta Part A: Molecular and Biomolecular Spectroscopy*

Received date: 29 September 2016
Revised date: 6 March 2017
Accepted date: 9 April 2017

Please cite this article as: Vengayil K. Harikrishnan, Sabeel M. Basheer, Nithin Joseph, Anandaram Sreekanth , Colorimetric and fluorimetric response of salicylaldehyde dithiosemicarbazone towards fluoride, cyanide and copper ions: Spectroscopic and TD-DFT studies. The address for the corresponding author was captured as affiliation for all authors. Please check if appropriate. Saa(2017), doi: 10.1016/j.saa.2017.04.007

Colorimetric and fluorimetric response of salicylaldehyde dithiosemicarbazone towards fluoride, cyanide and copper ions: Spectroscopic and TD-DFT studies

Vengayil K Harikrishnan, Sabeel M Basheer, Nithin Joseph and Anandaram Sreekanth*

Abstract

The sensing mechanism of salicyladehyde phenyldithiosemicarbazone (**SDTSC**) chemosensor has been investigated by spectroscopic and TD-DFT methods. The **SDTSC** shows colourimetric and spectral changes towards fluoride, cyanide and copper ions. The interaction between **SDTSC** with fluoride, cyanide and copper ions was examined through their absorption and fluorescence behaviour, and found that **SDTSC** has more sensing ability towards Cu^{2+} ion than CN^- and F^- ions. The ^1H NMR titration with **SDTSC** and F^- gives the structural changes in the sensing process. The reversibility of **SDTSC** was also evaluated and thus it is confirmed as a reusable chemosensor which can be clarified by the "Read-Erase-Read-Write" logic system. The DFT and TD-DFT calculations give the detailed sensing mechanism of **SDTSC** towards fluoride ion. The potential energy surface (PES) analysis confirms the excited state electron transfer mechanism.

Keywords: Dithiosemicarbazone; Spectroscopy; Chemosensor; Fluorescence; PES; TD-DFT

Department of Chemistry, National Institute of Technology, Tiruchirappalli - 620 015, India.

*Corresponding Author: E-mail address: sreekanth@nitt.edu; Tel: +91 431 2503642

1. Introduction

There is a growing interest in the development of appropriate sensors for the selective recognition of anions and cations, which play a vital role in the biological balance of the environment [1]. There is a high chance for human and other living beings to get exposed to the high level of these anions due to their immense use in the environment, which may lead to adverse or even fatal effects. Major challenges faced in this area of study is the development of structurally simple and stable receptor which is capable of achieving selective recognition of the anions and cations under consideration from the vicinity of a group of other anions and cations [2].

Fluoride ion having the smallest size and highest charge density attained much attention due to its importance in physiological processes and its presence in many environmental, food, and clinical samples. Beyond the Maximum Contaminant Level (MCL) established by the environmental protection agency >1.5mg/L, fluoride ions can cause many serious diseases such as dental and skeletal fluorosis, nephrotoxic changes and urolithiasis [3]. The detection of cyanide ion is also very important due to its potent toxicity. Cyanide ion is employed in many industrial processes such as fiber synthesis, resin synthesis, herbicide synthesis and gold extraction process [4]. This increased concentration of CN^{-} will also cause lethal effects in living beings. Transition metals are very important for the smooth functioning of biological activities. Among transition metals, Cu^{2+} ion is an essential trace element required for metabolism, respiration and enzymatic activities however in excess Cu^{2+} ions cause toxicity and degenerative memory related diseases. Due to its enormous use in all scientific fields' concentration of Cu^{2+} can go high which may lead to the destruction of biologically important microorganisms [5-6].

Most of the recent analytical techniques adopted for monitoring anions and cations are uneconomical, less sensitive, time consuming and tedious. The development of highly selective and sensitive chemosensors for the effective sensing of anions and cations will return high consistent results. The ability of the chemosensor to impart a visible colour change when in contact with the anions and cations will aid for the easy detection. UV-Vis and fluorescent analyses will provide apt supporting results with low cost and high sensitivity. The current work emphasises on the selective chemosensing activity of salicylaldehyde dithiosemicarbazone towards F^-, CN^- and Cu^{2+} and studying its mechanism both experimentally and computationally.

2. Experimental section

2.1 Materials and Methods

Phenyl dithiocyanate (Alfa), Salicylaldehyde (Aldrich) and tetra-n-butylammonium (TBA) salt of fluoride, chloride, bromide, iodide, perchlorate, phosphate, and acetate (Aldrich) were stored in vacuum desiccators containing self-indicating silica-gel and were used as received. Analytical grade DMSO and other solvents (Merck) were used without further purification. ^1H, and ^{13}C NMR spectra were recorded on a Bruker AVANCE III, 500 MHz in DMSO-d_6 at 298 K with TMS as an internal standard. FT-IR spectra were measured on a Perkin-Elmer FT-IR spectrometer using KBr pellets. UV–visible and fluorescence spectra were recorded in 1 cm path length quartz cell on PG Instrument T90 + spectrophotometer and JASCO FP-8300 spectrofluorophotometer, respectively.

2.2 Synthesis of receptor (SDTSC)

Ethanolic solutions (10 ml) of Phenyl dithiocyanate (0.250 g, 5mmol) and hydrazine hydrate (0.50 g, 10 mmol) were mixed with constant stirring. The Stirring was continued for one more hour. The product thus obtained was filtered, dried and recrystallized from ethanol. The obtained product (0.5 mmol) was mixed with salicylaldehyde (1 mmol) in DMF (15 ml). The mixture was stirred at 120^0C for 5 hours. The cold water was added to induce the precipitation of the product. The resulting precipitate was collected by filtration and washed with cold water. The resultant product was dried in an oven at 110 ^0C.

SDTSC: Light green; Yield: 89 %, **M.P.**: 180-188^o C; **Elemental analysis**: C: 56.53 (56.88), H: 4.89 (4.34), N: 17.84 (18.09), S: 13.57 (13.80); **IR** (cm^{-1}): 1542 (C=N), 1271(C=S), 3153(NH), 3383(OH); **^{1}H NMR** (500 MHz, DMSO-$d_{6,}$ δ ppm): 11.778 (1H, s, OH), (11.134 (1H, s, N-NH), 10.07 (d, J = 24.5 Hz, 2H), 9.982 (1H, s, N=CH), 8.50-6.85(12H, m, Ar-H), **^{13}C NMR** (125 MHz, DMSO-$d_{6,}$ δ ppm): 162.77(1C,C=S), 139.78 (C=N), 130.82(C=C), 99.49 (C-OH); **ESI MASS**: 464.56 (Calculated), 464.10 (Experimental) (M+, 100%), 487.10 (base peak-M+Na)

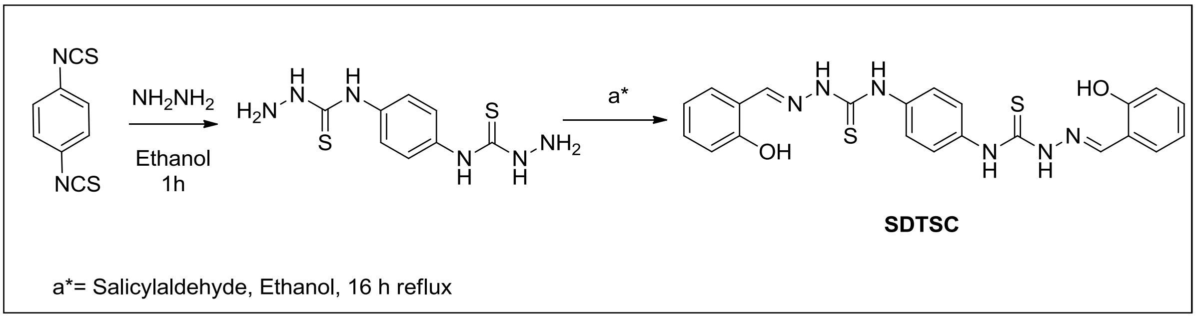

Scheme 1: Synthesis of salicylaldehyde based phenyldithiosemicarbazone ligand

2.3 UV-visible and fluorescence titrations

The binding ability of the **SDTSC** for anions and cations was investigated through UV-visible and fluorescence titration methods. The **SDTSC** (1×10^{-6} mol. L^{-1}) as well as salts of anions (such as F^-, Cl^-, Br^-, I^-, CN^-, $H_3PO_4^-$, AcO^-, NO_3^-, HSO_4^- and OH^-) and cations (such as Mn^{2+}, Co^{2+}, Cu^{2+}, Cr^{3+}, Fe^{2+}, Ni^{2+} and Zn^{2+}) were prepared in DMSO. Two equivalents of anions and cations were added to the receptor solution and their corresponding UV-visible and fluorescence spectra were recorded at 298 K.

2.4 Computational Methods

All computational calculations were executed using Gaussian 09 program. The Time Dependent DFT (TD-DFT) and hybrid density functional theory (DFT) calculations were performed to optimize the ground state and excited state structures of **SDTSC** and its complex with F^- and Cu^{2+} [7-10]. The ground state geometry of **SDTSC** and **SDTSC**–F complex was optimized using B3LYP/6-31G+(d,p) basis set, which helped to evaluate the hydrogen transfer transition state calculations. The excited state energy calculations were performed using Coulomb-attenuating method (CAM) with a long-range corrected version of B3LYP for more accuracy. The calculations of **SDTSC–Cu** complex were carried out with B3LYP/LanL2DZ method [10-13]. The UV-visible transition studies were examined using TD-DFT method starting with ground state geometries optimized in DMSO solution phase with PCM model. The potential energy surface (PES) gives information about the distribution of electron density in atoms and in bonds between atoms.

3. Results and Discussions

The structural formula of **SDTSC** is as shown in **Scheme 1**. It was well-characterized by elemental analyses, FT-IR, ^{1}H NMR, ^{13}C NMR and ESI MASS spectral studies. The electronic spectra of the compound exhibited two bands around 303 and 345 nm, which were characteristic of $\pi\rightarrow\pi^*$ and $n\rightarrow\pi^*$ transitions respectively. The FT-IR spectrum of the compound express the characteristic stretching frequencies at 1271 and 1542 cm^{-1} attributed to ν(C=S) and ν(C=N) groups respectively, which indicates the newly formed azomethine group. Also SDTSC showed a characteristic band at 3383 cm^{-1} which were assigned to ν(N−H) group. The ^1H NMR of the **SDTSC** displays singlet at 11.134 and 9.932 ppm for two different N-H protons respectively. The peak at 11.778 ppm related to the hydroxyl proton. The aromatic protons were in the expected range of 8.50-6.85 ppm. The ^{13}C NMR spectra of the compound shows the thiocarbonyl (C=S) and imine (C=N) carbon peaks at 162.77 and 139.78 ppm respectively.

3.1 Colorimetric analysis and UV-visible spectral studies

The **SDTSC** shows two principal absorption peaks at 303 and 345 nm which corresponds to $\pi\rightarrow\pi^*$ and $n\rightarrow\pi^*$ transitions respectively. The absorption properties of **SDTSC** significantly vary due to the interaction with selective anions and transition metals. When a solution of **SDTSC** is treated with various anions (such as F^-, Cl^-, Br^-, I^-, CN^-, $H_2PO_4^-$, AcO^-, and NO_3^- as tetrabutylammonium salts) and transition metals (such as Mn^{2+}, Ca^{2+}, Cu^{2+},Co^{2+} , Cr^{3+}, Fe^{2+}, Ni^{2+}, and Zn^{2+}), the absorption profile as in **Figure 1** was obtained [15-17] . On addition of F^- and CN^- ions to the **SDTSC**, the colour of the solution changes from colourless to light mustard yellow and deep mustard yellow respectively. The addition of Cu^{2+} produces a deep yellow colour, but with other anions and cations there is no observable colour change even on excess addition **(S1).** The absorption spectral changes of **SDTSC** towards F^-, CN^- and Cu^{2+} ions were observed through spectrometric titrations. The presence of F^- and CN^- ions result in the formation of new peaks at 394 and 465nm, the absorbance of the bands gradually increased due to the incremental addition of the ions. The generation of the new peak is due to the complexation between the host-guest molecules via mere hydrogen bonding. Simultaneously, the hypochromic shift happened at 394 nm, along with a red shift and a 49 nm difference. This infers that the **SDTSC**–F complex has more π-conjugation than **SDTSC** alone. The isosbestic point was observed at 372 nm, which implies the presence of multi-ions in the solution. The presence of Cu^{2+} in the **SDTSC** results in the formation of a new peak at 410 nm, the absorbance of this peak proportionally increased with increase in the concentration of the copper ion [18-21]. The UV-Vis spectral profile of F^-, CN^- and Cu^{2+} with **SDTSC** is as shown in **Figure 2**.

Job's Method also known as the method of continuous variation, is a simple and efficient method to measure the chemical reaction stoichiometry. From the Job’s plot, it is clear that the receptor was bonded with fluoride, cyanide ions in 1:2 ratio and copper ions are in 1:1 ratio (see **S2**). The association constant of **SDTSC** with F^-, CN^- and Cu^{2+} ions was calculated using Benesi-Hilderband equation, which is as below [18], [22],

$$\frac{1}{A-A_0}=\frac{1}{A_\infty-A_0}\left[\frac{1}{K[ion]}+1\right]$$

where 'A_0' is the absorbance of the free receptor , 'A' is the absorbance with a specific fluoride ion concentration , 'A_∞' is the absorbance with an excess amount of ions (F^-, CN^- or Cu^{2+}), 'K' is the association constant (M^{-1}). **S3** shows a linear relationship between $1/(A - A_0)$ *vs* 1/[ion], and association constant (K_a) found to be 2.007 x 10^4, 4.006 x 10^4 and 6.792 x 10^4 M^{-1} for F^-, CN^- and Cu^{2+} respectively. From that, it is clear that the **SDTSC** has a more binding affinity towards Cu^{2+} than F^- and CN^- ions.

3.2 Fluorescence spectral studies

To study the fluorescence behaviour of **SDTSC** towards anions and transition metals, the fluorescent emission titrations were carried out with anions (such as F^-, Cl^-, I^-, Br^-, AcO^-, NO_3^-,ClO_4^-, HSO_4^- and $H_2PO_4^-$) and transition metals (such as Mn^{2+}, Fe^{3+}, Co^{2+}, Ni^{2+}, Cu^{2+} and Zn^{2+}). The **SDTSC** shows an emission peak at 458 nm, when it is excited at 400 nm. As shown in **Figure 3** and **Figure 4**, **SDTSC** exhibited a remarkable alteration in the emission band at 394 and 465 nm in the presence of F^- and CN^- respectively. Addition of Cu^{2+} to **SDTSC** gives continuous quenching of emission intensity at 458 nm. The emission intensity decreased due to the gradual increase of copper ion concentration. This experimental change in emission causes quenching, which is due to the formation of a new Cu-complex. There is no other fluorescence was observed from the receptor with the other anions rather than F^- and CN^-. In the case of cations the quenching is maximum with Cu^{2+} while comparing with the other metal ions and it. Also a similar quenching has also occurred with Co^{2+} and Fe^{3+}. So in that logic the quenching behaviour is not selective to Cu^{2+}. The detection limit was calculated based on the fluorescence titration. To determine the S/N ratio, the emission intensity of receptor without any analyte was measured 10 times. The equation [(LOD)=K x (δ/S)] was used to calculate the limit of detection of receptor towards F^-, Cu^{2+} and CN^- ions, where $\delta=\sqrt{\frac{\sum (F_0-F)^2}{N-1}}$, ($F_0$, F are fluorescence intensity of receptor alone and addition of ion respectively. 'N' is the number of equivalence). The constant 'K' = 3 in this case and σ =

(Sb1)/(S); Sb1 is the standard deviation of the blank solution; S is the slope of the calibration curve. The limit of detection of receptor towards fluoride, cyanide and copper ions were 0.974x10^{-7}, 0.348x10^{-7} and 0.7394x10^{-7} M respectively. Hence, the **SDTSC** shows more sensing towards fluoride ion than copper and cyanide ions. This value is far below the guideline (211 μM) of the U.S Environment Protection Agency. The limit of detection graphs were as shown in **S4**.

3.3 ^{1}H NMR titration studies

The mechanism of the interaction between **SDTSC** and F^- was further studied by ^{1}H NMR spectroscopy in DMSO-d^6. The ^{1}H NMR titration leads to the studies in structural changes during the complexation between **SDTSC** and fluorine ion and thus showing observable changes in the spectra. The O–H, N_1–H_1 and N_2–H_2 protons of **SDTSC** appeared as a sharp singlet at 11.01, 8.8 and 6.7 ppm respectively. With the addition of F^- ion to the **SDTSC**, the peak at 11.01 ppm completely disappeared. While, the intensity of the signals at 8.8 and 6.7 ppm was decreased, and disappeared with the excess addition of F^- ion. The results show, the first deprotonation occurs from the hydroxyl group of **SDTSC**. The upfield shifting is due to the aromatic protons which implies that the negative charges generated from the deprotonation of the receptor by fluoride ion was delocalized over the **SDTSC**. Two stepwise mechanism happens during the formation of hydrogen bond between the hydroxyl group (O–H) and F^- and deprotonation of O–H by excess addition of F^-. This suggests the interaction of $F_1{\cdots}H{\cdots}O$ protons and excess fluoride leads to the deprotonation of the moiety. The broadness of the peaks at 8.8 and 6.7 ppm indicates the formation of hydrogen bonding via $N_1{\cdots}H_1{\cdots}F_2$ and $N_2{\cdots}H_2{\cdots}F_2$. Hence resulting in the sensing mechanism of F^- and SDTSC which is due to intermolecular hydrogen bond, deprotonation, and π-conjugation effect. The ^{1}H NMR spectra shown in **Figure 5**.

3.4 Reversibility of SDTSC

The reversible property is an important aspect for a chemosensor and to be broadly hired in the recognition of specific analyses, so the reversibility in the response of the **SDTSC** has been further confirmed during several cycles of titration by the alternate addition of F^- and Ca^{2+} to the **SDTSC** solution. The addition of F^- results in significant fluorescence change by displaying an ‘ON’ behaviour through **SDTSC**–F complex formation. The addition of Ca^{2+} to the **SDTSC**–F mixture results in the quenching of fluorescence intensity, which refers to ‘OFF’ behaviour. A few efficiency loss of fluorescence intensity cause the

"OFF-ON-OFF" switching process which repeats for several times [27]. This repeated behaviour of the scheme by fluorescence change evidently proposes that **SDTSC** is reversible and thus reusable. The conceivable scheme as presented in **Figure 6**. The results attribute to the "Read-Erase-Write-Read" character with the support of logic operations. Thus a model of the truth table input and output of the suggested logic circuit has been conceded effectively and summarized as shown in **Figure 7 [27]**.

3.5 Computational Studies

3.5.1 Geometry optimizations

The comparison of the optimized excited structures with ground state structures give the idea of the excited state proton transfer process (ESPT) and inter charge transfer process (ICT). **S5** displays the optimized structures of the **SDTSC**, fluoride ion complex (**SDTSC**–F), copper ion complex (**SDTSC**–Cu) and deprotonated receptor (de-**SDTSC**). The observed bond parameters were listed in **S7**. In the ground state of **SDTSC**, the dihedral angle between cyclohexane group and thiosemicarbazone group (C_3–N_3–C_2–S_1) is 8.2^0, which attributes that SDTSC has no coplanarity in the ground state. But in **SDTSC**–F complex, the dihedral angle reduces to 5.67^o and the deprotonated receptor (de-**SDTSC**) has a coplanar structure (dihedral angle is zero).The planarity gives photoirradiation when the fluoride ion binds with the receptor. The O–H bond in **SDTSC** and **SDTSC**–F are 0.96 and 1.41 Å respectively, which implies that the deprotonation happened in the ground state of the R1-F complex. The calculated bond distance of N_1–N_2, C–N and C_2=S_1 in **SDTSC** are 1.35, 1.38 and 1.66 Å respectively. While in the optimized structure in the ground state and the excited state of **SDTSC**–F, the bond lengths slightly increase when compared to **SDTSC** (see Table 1). The formation of fluoride ion complex is an intermediate stage and fluoride anion interrelates through hydrogen bond interaction. In the ground state of **SDTSC**–F, the dihedral angle between N_1–N_2–C_2–S_1 and cyclohexyl-thiosemicarbazone groups are 6.64 and 5.672^0 respectively. The thiocarbonyl group (C=S) bond distance remains same in ground state and excited states of **SDTSC** and **SDTSC**–F. The dihedral angle between thiosemicarbazone moiety and phenyl moiety creates the planar structure of C_3-N_3-C_2-S_1 in the ground state, which twists to 5.67^0 for the excited state structure of **SDTSC** and thus the photoirradiation happened. The dihedral angle is twisted to 5.672^0 in the excited state of **SDTSC**–F, and their planarity is lost. In **SDTSC**–F, the bond distance between N_2-H_5 and N_3-H_6 are higher than **SDTSC**, which is further increasing in the excited state of **SDTSC**–F. The bond distance of O_1–H_{14} and N_2-H_5 in the excited state of **SDTSC**–F is not enough to form the bond, hence it clear that the deprotonation happened in the excited state. So it is strongly verified that the hydrogen is detached from N_2, which is close to thiosemicarbazone moiety and not from the nitrogen neighbouring to the cyclohexyl group (N_3). The deprotonation causes the exclusion of the hydrogen at the excited state. Finally, the results concluded that the intermolecular excited-state proton transfer (ESPT) will happen in an excited state in the presence of fluoride anion. In the **SDTSC**–Cu complex, the prominent difference of bond parameters in the ground state was evaluated, which exposes that the copper binding took space in the ground state. The Cu-O, Cu-S and Cu-N bond distances are 1.93, 2.30 and 2.07 Å respectively. The C=S bond distance in **SDTSC** and **SDTSC**–Cu were found to be 1.66 and 1.81 Å respectively, which implies that a single bonded C–S in **SDTSC**–Cu complex. There is no observable variation in the bond parameters at ground state and excited state and so the binding took place at the ground state.

3.5.2 UV-visible spectra and molecular orbital analysis

The absorption behaviour of the receptor in sensing of fluoride ions was investigated with the help of molecular excitation study. The **SDTSC** gives a strong absorption peak at 329 nm with 1.0425 oscillating strength, which attributes the $\pi\rightarrow\pi^*$ transition from the highest occupied molecular orbital (HOMO) to the lowest unoccupied molecular orbital (LUMO).The comparison of absorption spectra for **SDTSC** and **SDTSC**–F complex have been conducted to recognize the sensing mechanism. The molecular orbitals involved in the main electronic transitions have been shown in **Figure 8** and **S8**. The intense transition for **SDTSC**–F is at 305 nm, and it is assigned to the $\pi\rightarrow\pi^*$ transition from the highest occupied molecular orbital (HOMO) to lowest unoccupied molecular orbital (LUMO) and the second highest occupied molecular orbital (HOMO-1) to LUMO with 4.06 ev energy gap. The **SDTSC**–Cu complex shows $\pi\rightarrow\pi^*$ transition between HOMO to LUMO at 559 nm. The major electronic transitions are HOMO-2 to LUMO at wavelength 726 nm, and the larger oscillating strength is at 559 nm, which is HOMO to LUMO transition.

3.5.3 Potential energy curves (PES)

To further clarify the excited state proton transfer mechanism (ESPT) process in the fluoride sensing mechanism of **SDTSC**, the potential energy surface calculations were carried out for the ground state and excited state of **SDTSC**–F and **SDTSC**–Cu complexes. In **SDTSC**–F, the bond distance between F–H and O–H varies from 0.90 to 1.8 Å with 0.05 Å increment. This speculate the energetic pathway for ESPT process that is described from this calculation. It is clearly interpreted from **S6** that the energy of excited state for **SDTSC**–F decreases on elongation of the O–H bond length, and it increases through a stable point about 1.2 Å, and leads to a geometry for the stable excited state. Consequently, the fluoride atom chooses to capture proton from O–H donor to form an intermolecular hydrogen bond. Therefore the addition of the fluoride anion enhances the spontaneous ESPT process in the excited state of the proton transferring from oxygen atom to fluoride atom [17], [18].

4. Conclusion

The **SDTSC** was synthesized systematically and the fluorescence sensing properties of dithiosemicarbazide for anions and cations were studied by various optical and spectroscopic techniques. **SDTSC** showed visible colour changes and observable fluorescence change towards fluoride, cyanide and copper ions. The deviations in absorption and fluorescence spectra were observed, ^{1}H NMR studies established the sensing mechanism. The NMR titration showed that the hydroxyl group underwent deprotonation. The NH proton next to the hydroxybenzylidene, was deprotonated by further addition of F^-. It was seen that a hydrogen bond was formed between them. The evaluated binding constants confirms that **SDTSC** has more binding affinity towards fluoride, cyanide and copper ion. The sensing process was investigated with computational calculations using DFT and TDDFT methods. The outcomes of computational studies led to the important aspects of the interaction between **SDTSC** and F^-/Cu^{2+}. This also predicted the mechanism of sensing. The fluoride sensing process took place at the excited state of **SDTSC**–F complex, via deprotonation followed by the hydrogen bond formation. The PES calculations confirm the excited state proton transfer of **SDTSC**. The reversibility of **SDTSC** was checked with the alternative addition of Ca^{2+} and F^-, which was seen to be reversible. Hence making **SDTSC** a reusable chemosensor. The computational calculations well replicated the experimental UV-vis and fluorescence spectra results.

REFERNCES

[1] E. Katayev, A. Ustynyuk, Y.A. J. L. Sessler, Coord. Chem. Rev. 250 (2006) 3004-3037.

[2] L. Gaia, J. Mack, H. Lua, T. Nyokong, Z. Li, N. Kobayashi, Z. Shen, Coord Chem Rev. 285 (2015) 24-51.

[3] J. Liu, Juan, X. He, J. Zhang, T. He, L. Huang, J. Shen, D. Li, H. Qiu, S. Yin, Sens. Actuat. B; Chem. 208 (2015) 538-545.

[4] R. Kavitha, T. Stalin, J. Lumin. 158 (2015) 313-321.

[5] Y.J. Na, Y.W. Choi , J.Y. Yun , K.M. Park , P.S. Chang, C. Kim, Spectrochim. Acta Part A Mol. Biomol. Spectrosc. 136 (2015) 1649-1657.

[6] T.G. Jo, Y.J. Na, J.J. Lee, M.M. Lee, S.Y. Lee, C. Kim, Sens. Actuat. B; Chem. 211 (2015) 498–506.

[7] M. E. Casida, C. Jamorski, K.C. Casida, D.R. Salahub, J. Chem. Phys., 108 (1998) 4439-4449.

[8] R.E. Stratmann, G.E. Scuseria, M.J. Frisch, J. Chem. Phys., 109 (1998) 8218-24.

[9] R. Bauernschmitt, R. Ahlrichs, Chem. Phys. Lett., 256 (1996) 454-64.

[10] S.L.A. Kumar, M.S. Kumar, R.P. John, P. T. Muthiah, A. Sreekanth, Mater. Sci. Eng., C. 33 (2013) 2519-2525.

[11] T. Yanai, D. Tew, N. Handy, Chem. Phys. Lett., 393 (2004) 51-57.

[12] G. Zhao, K. Han, Comput. Chem., 29 (2008) 2010–2017.

[13] B. Miehlich, A. Savin, H. Stoll, H. Preuss, Chem. Phys. Lett., 157 (1989) 200–206

[14] C. Peng, P.Y. Ayala, H.B. Schlegel, M.J. Frisch, J. Comp. Chem., **17** (1996) 49

[15] M.S. Kumar, S.L.A. Kumar, A. Sreekanth, Anal. Methods. 5 (2013) 6401-6410.

[16] S.M. Basheer, N.S.P. Bhuvanesh, A. Sreekanth, J. Fluorine Chem. 191 (2016) 129-142.

[17] S.L.A. Kumar, R. Tamilarasan, M.S. Kumar, A. Sreekanth, Ind. Eng. Chem. Res. 50 (2011) 12379-12383.

[18] S.M. Basheer, A.C. Willis, R.J. Pace, A. Sreekanth. Polyhedron, 163 (2016) 7-18.

[19] S.M. Basheer, A. Sreekanth, Comp. Theor. Chem. 1085 (2016) 31-39.

[20] S.M. Basheer, A.C. Willis, A. Sreekanth, J. Lumin. 183 (2017) 266-280.

[21] R. Sivakumar, V. Reena, N. Ananthi, M. Babu, S. Anandan, S. Velmathi, Spectrochimi. Acta Part A Mol. Biomol. Spectrosc. 75 (2010) 1146-1151.

[22] A. Sreekanth, H.K. Fun, M.R.P. Kurup, J. Mol. Struct. 737 (2005) 61-67.

[23] L.I. Bruijn, T.M. Miller, D.W. Cleveland, Annu. Rev. Neurosci., 27 (2004) 723.

[24] Satheshkumar, E.H. El-Mossalamy, R. Manivannan, C. Parthiban, L.M. Al-Harbi, S.Kosa, K.P. Elango, Spectrochim. Acta, Part A. 128 (2014)798-805

[25] T.Gunnlaugsson, M. Glynn,G.M. Tocci,P. E. Kruger, F.M. Pfeffer, Coord. Chem. Rev. 250 (2006) 3094–3117.

[26] B. Sen, M. Mukherjee, S. Banerjee, S. Pal, P. Chattopadhyay, Dalton Trans. 44 **(**2015), 8708-8717.

[27] G.T. Yan, H. Li, Y.R. Zhu, B. Shi, W. Qu, Q. Lin, H. Yao, Y. Zhang, T. Wei, New J. Chem. 39 (2015) 8797-8801.

[28] V.K. Gupta, S. K. Shoora, L. K. Kumawata,A. K. Jain, Sens. Actuators B. 209 (2015) 15–24.

[29] A. Caballero, F. Zapata, P.D. Beer, Coord. Chem. Rev. 257 (2013) 2434– 2455.

[30] J.S. Chen, P.W. Zhou, L. Zhaoab, T.S. Chu, RSC Advances. 4 (2014) 254-259.

[31] P. Ghosh, B.G. Roy, S. Jana, S.K. Mukhopadhyaye, P. Banerjee, Phys. Chem. Chem. Phy. 17 (2012) 20288-20295.

[32] G.Y. Li, T. Chu, Phys. Chem. Chem. Phys. 13 (2011) 20766-20771.

[33] G.Y. Li, J.P. Wang, H. Zhang, W.W. Li, F. Wang, Y.H. Liang, Chem. Phys. Lett. 616 (2014) 30-34.

[34] J.S. Chen, P. Zhou, G. Li, T.S. Chu, G. He, J. Phys. Chem. B. 17 (2013) 5212-5221.

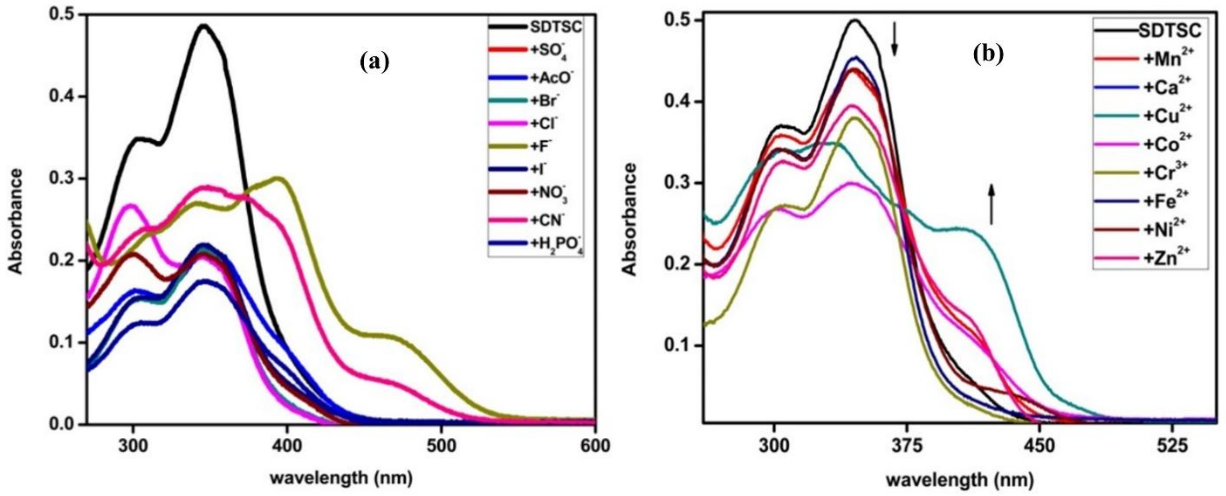

Figure 1: UV Vis spectra of SDTSC with different concentration of (a) anions and (b) cations.

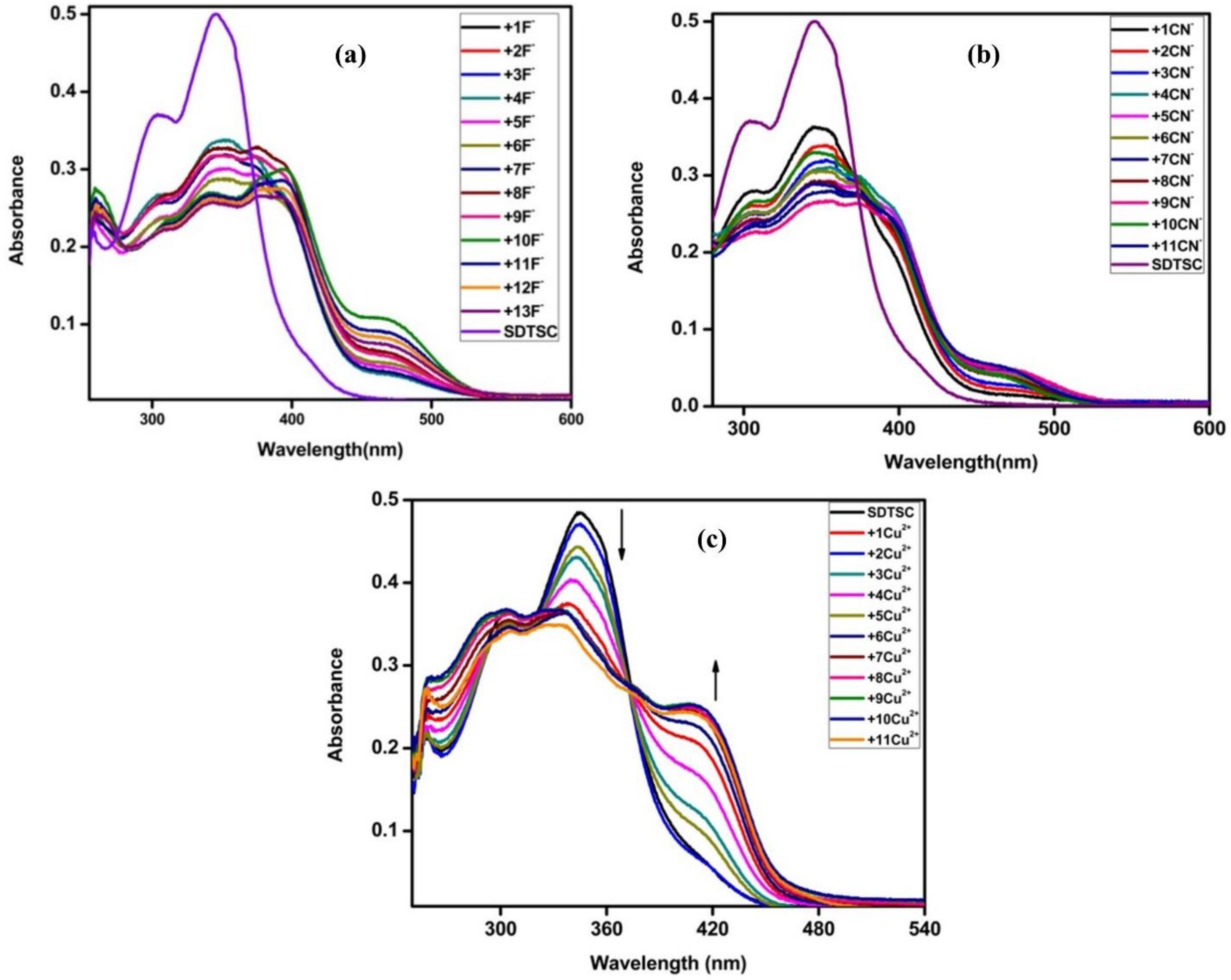

Figure 2: UV Vis titration spectra of receptor SDTSC with (a) fluoride and (b) cyanide (c) copper ion.

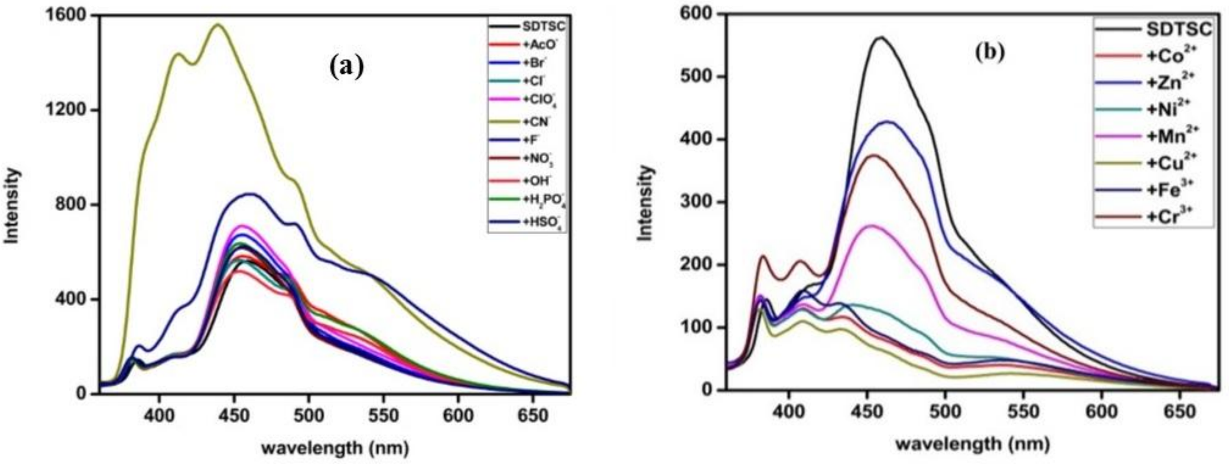

Figure 3: Emission spectra of receptor SDTSC with different (a) anions and (b) cations.

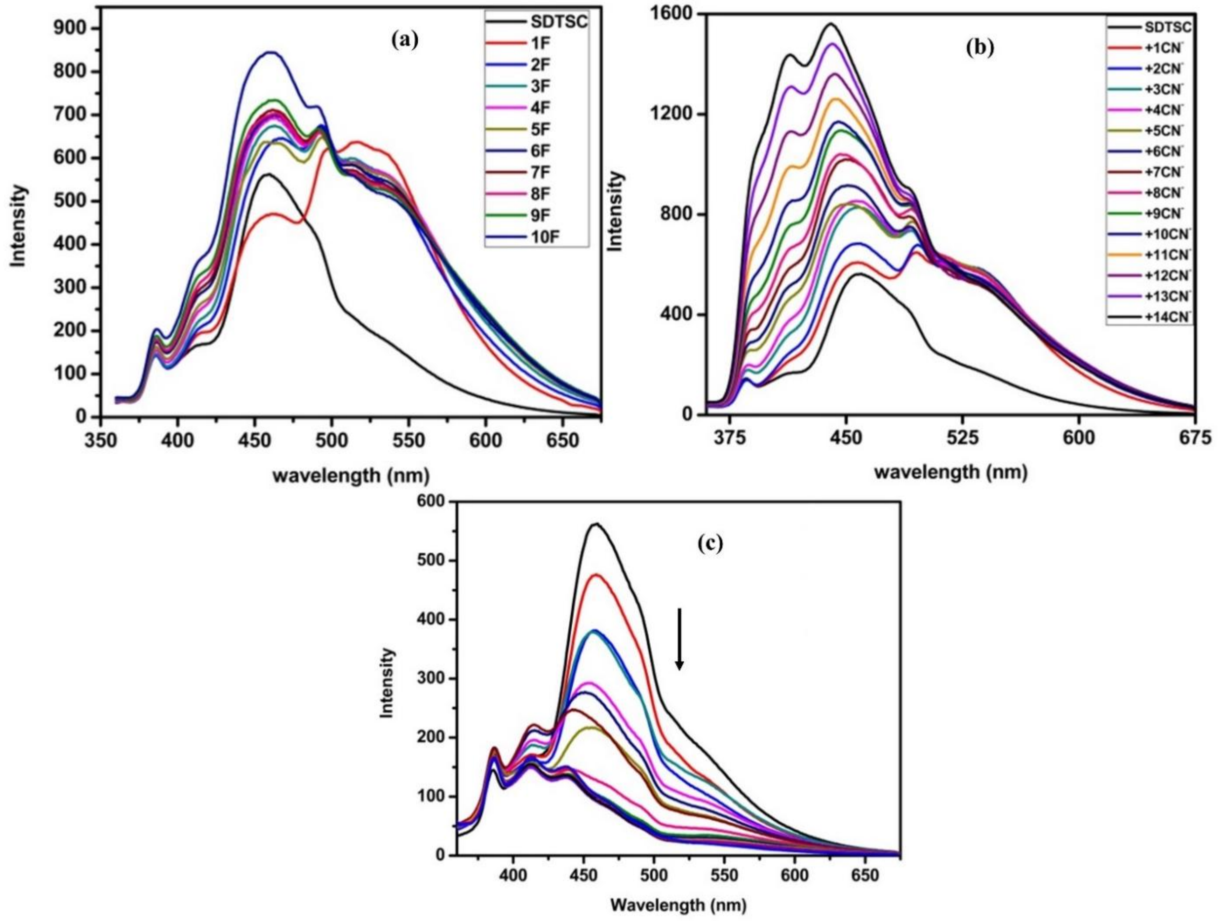

Figure 4: Emission titration spectra of receptor SDTSC with (a) fluoride and (b) cyanide ion.

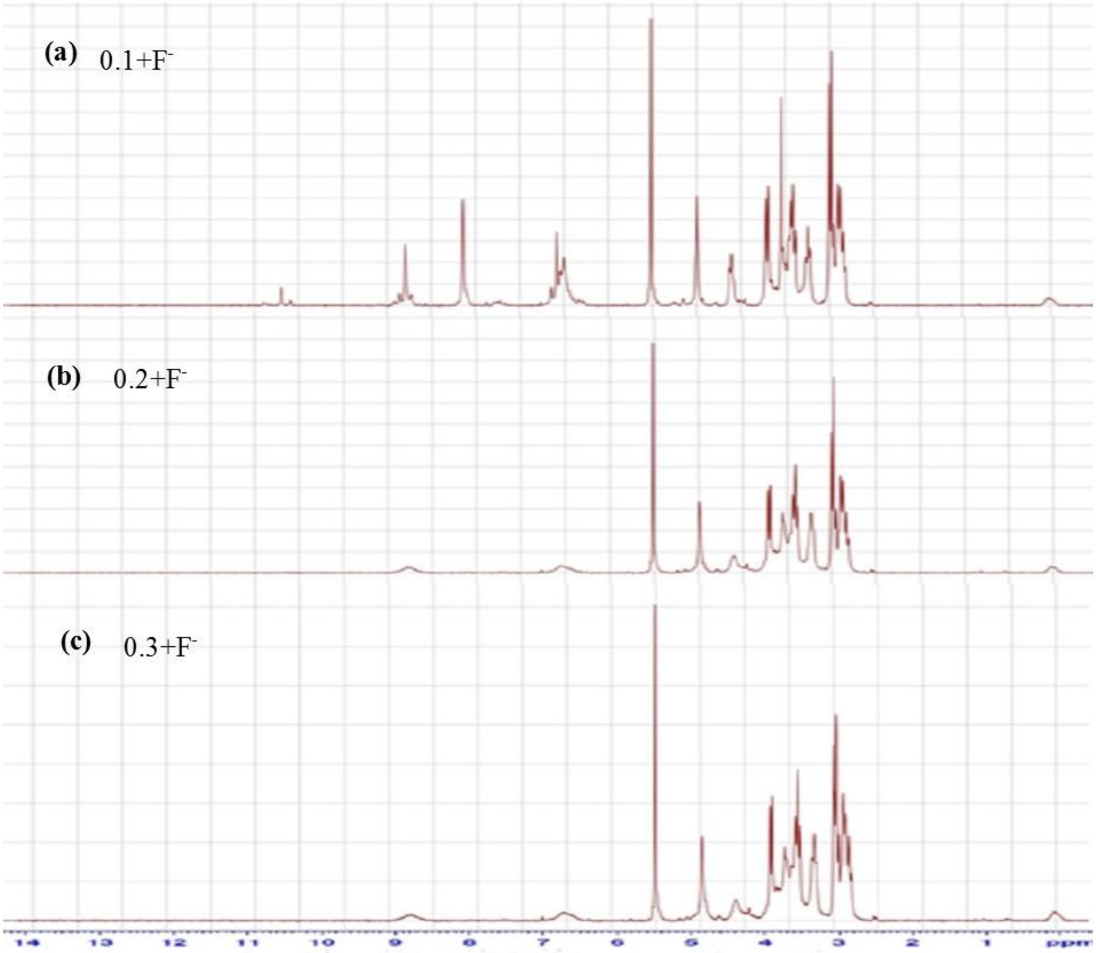

Figure 5: ^{1}H NMR titration data of SDTSC with F$^-$ ion.

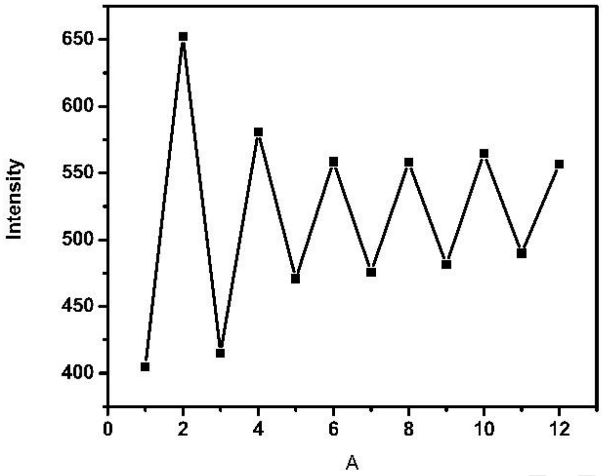

Figure 6: Reversible switching cycles of SDTSC with fluorescence intensity (λ_{ex}=458 nm) by alternate addition of F^- ions and Ca^{2+}.

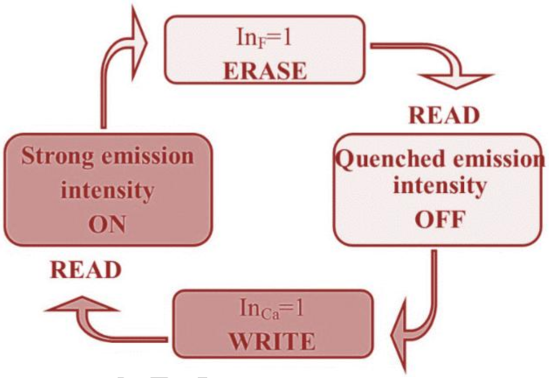

Figure 7: Feedback loop showing reversible logic operations for memory element with “Read-Erase-Write-Read” functions.

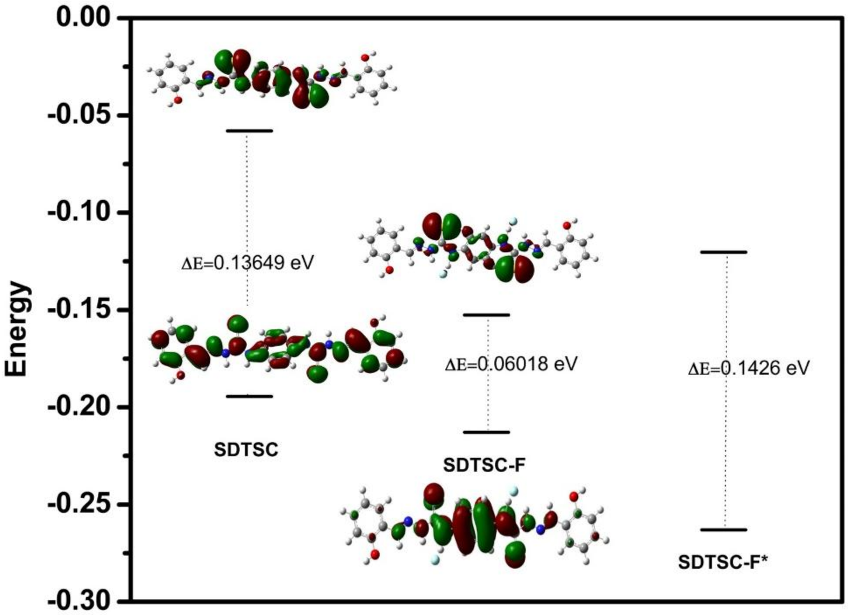

Figure 8: The energy gap between HOMO to LUMO orbitals contributed to the transition for SDTSC and SDTSC-F.

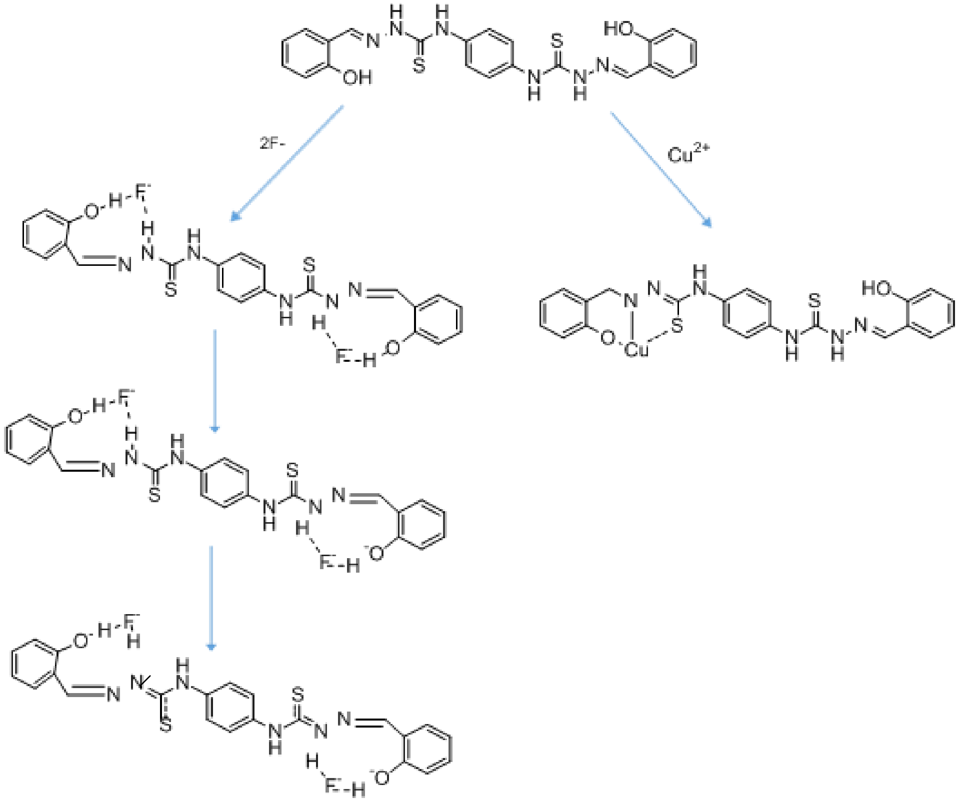

Figure 9: The sensing binding mode and mechanism of SDTSC towards fluoride and copper ions

Table 1: Association constant of SDTSC with Fluoride. Cyanide and Copper

Ions	**UV-vis spectra** **K_a**
Fluoride ion	2.007×10^4
Cyanide ion	4.006×10^4
Copper ion	6.792×10^4

Graphical Abstract:

A schematic representation of molecular switching mode of **SDTSC** towards copper and fluoride/cyanide ions with the alternative addition of corresponding ions.

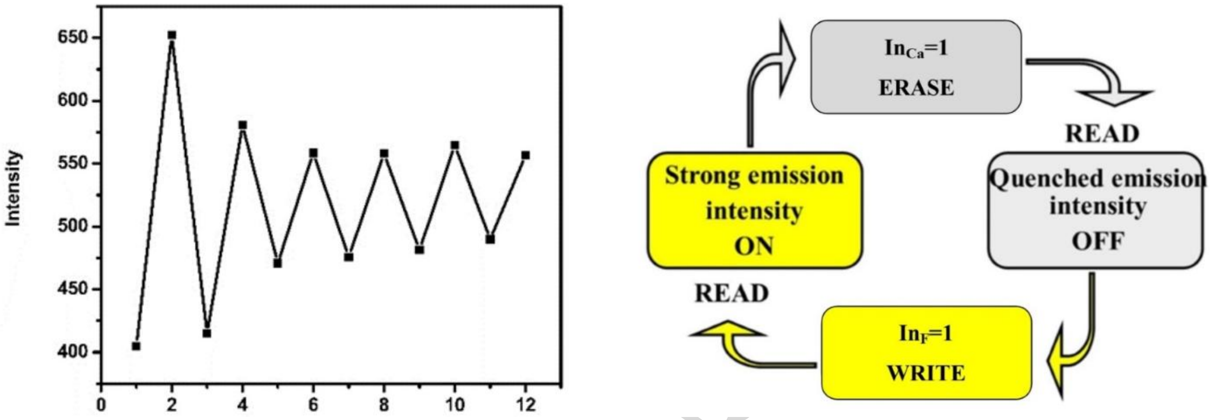

Highlights

- Synthesis and characterization of dithiosemicarbazone derivative
- Experimental evolution of selective fluoride, cyanide and copper sensing via both colorimetric and spectroscopic studies
- Fluoride ion sensing mechanism was proposed using experimental and DFT/TDDFT methods
- The multi-detection of receptor was used to describe the molecular switching behavior.